

## Dielectronic recombination in plasmas: The final state distribution

Gaber Omar

*Physics Department, Ain Shams University, Abbasia, Cairo, Egypt*

Yukap Hahn

*Department of Physics, University of Connecticut, Storrs, Connecticut 06269*

(Received 22 November 1999)

The dielectronic recombination rate is one of the important input parameters to rate equations for modeling plasmas, where the excited state population of the plasma ions is determined by taking into account the radiative and collisional effects of plasma particles. The rates are often conveniently summarized in the form of empirical formulas to facilitate their use; in particular, properly designed rate formulas are needed that describe the electron capture to the individual singly excited final recombined states. However, the currently available rate formulas fail to meet this requirement, although they are obtained from more detailed benchmark calculations that explicitly include all the important transitions. The modified rate formulas may be obtained by keeping separate the rates to the individual singly excited final states, but still summing the contributions from different intermediate resonance states, with proper account of the cascades. Ne-like  $Al^{3+}$  ions in their ground state are used as examples to show that the rates to the final ground state are reduced by as much as a factor of 5 from the total rates.

PACS number(s): 52.20.-j, 34.80.Kw, 32.80.Dz

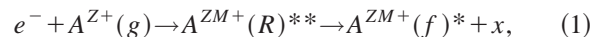
### I. INTRODUCTION

The importance of the dielectronic recombination (DR) process in the analysis of line spectra emitted by astrophysical plasmas and the realization in the 1970s that DR by impurity ions in tokamaks is the dominant cooling mechanism have been the main incentive for much of the research activity on DR in recent years, both experimentally and theoretically [1,2]. For highly charged ions, heavy-ion accelerators with storage rings and electron-beam ion traps have played an especially important role in generating experimental data, while for low-charged ions large effects of electric fields on DR have been observed experimentally [3].

DR is one of the three known ways by which plasma electrons recombine with ions. The other two are radiative recombination (RR) and three-body recombination (TBR). The excess energy released by the recombining electrons is carried away by emitted photons in RR and by increased kinetic energy of the participating electrons in TBR. On the other hand, in DR the energy released by the recombining electron is first expended to excite one of the bound electrons of the target ion. This first step of excitation recombination does not involve radiation, but creates a doubly excited autoionizing state, which can subsequently decay either radiatively to singly excited final states ( $f$ ) of the recombined ion, or to the initial state via inverse autoionization. If states reached by radiative emission are still multiply excited and Auger unstable, then further cascade corrections must be applied until Auger-stable final states are reached, thus completing the DR, although the states may still be radiatively unstable. In the absence of plasma perturbations, the Auger-stable final excited states  $f$  may be summed to obtain the total DR rates. However, the presence of plasma particles can modify their population, and this is what a modeling program needs to determine. Consequently, the excited state distribution resulting directly from the DR process is important

as an input to the rate equations.

In the simplified independent electron picture, the two-step DR process of excitation/capture followed by a radiative decay to Auger-stable final states is schematically described by



where  $g$  is the ground state of the target ion with charge  $Z$ ,  $R=(a,b)$  are doubly excited resonance states of the recombined ion of charge  $ZM=Z-1$ , and  $f$  is the final state of the recombined ion in a singly excited state with the principal quantum number  $n$ . In Eq. (1),  $x$  denotes the emitted radiation. In the single-particle picture, the excitation energy  $\Delta_{ag}=e_a-e_g$  is supplied by the recombining electron as it releases the excess energy  $\Delta_{cb}=e_c-e_b=\Delta_{ag}$ . Thus, the initial step of excitation/capture makes DR a resonant process with sharp dependence on the continuum electron energy  $e_c$ .

In modeling plasmas, a set of rate equations is constructed for the population distribution  $N(n)$  of excited states ( $f$ ) of the recombined ion, where the equations are to describe the various effects of the plasma particles (both electrons and ions) on these excited states as the system approaches a quasi-thermal equilibrium. Because of the large number of rates needed in modeling, the rates are usually summarized in a simple set of empirical rate formulas, as obtained from detailed calculations. While the empirical rates that describe processes such as RR, TBR, collisional ionization and excitation, etc. explicitly specify the individual final excited states, the currently available DR rate formulas fail to conform to this requirement. They are in most cases the total rates obtained by summing the contributions from all the final singly excited states  $f$ , as well as from all the intermediate resonance states  $R$ . When summed over  $f$ , the valuable information given by detailed benchmark calculations is lost. Thus, no explicit dependence of the rates on the final states is

present. Consequently, the total rates are often used as though the only DR contribution is to the “ground” states of the ions after the recombination. Such a procedure is obviously not consistent, and can be justified only when the process takes place in isolation or at low plasma densities, where the effect of the plasma environment is negligible. Then, eventually states  $f$  will, by the definition of Auger stability, relax radiatively to the ground states of the recombined ions. But in a plasma where many electrons and ions are present, the states  $f$  are often strongly perturbed, and it is precisely the task of plasma modeling to implement this perturbation via a set of rate equations.

It is the purpose of this report first to point out the deficiency in the currently available rate formulas, and to show that, when the final excited state dependence of DR is explicitly retained, the rates for the final ground states  $f_0$  of the recombined ions are greatly suppressed. The amount of work involved in benchmark calculations is increased slightly when the contributions to the individual  $f$  states must be collected state by state, but the data to be cataloged are now increased manyfold. How to summarize these newly adjusted data in a convenient set of empirical formulas is a question yet to be addressed. Exceptions to this deficiency are the modeling studies in which detailed rates obtained from the explicit calculations, and not from the empirical formulas, are used directly in the rate equations. However, most of the huge modeling codes use the simple empirical formulas. Furthermore, as stressed previously [4], the rate equations and the input rates presumably provide a complete description of the plasma relaxation toward equilibria. Therefore, approximations introduced in constructing the rate equations must be compensated by the input rates, and vice versa. For practical reasons, the approximate set of rate equations chosen is often finite in number, with an upper cutoff at states that are rapidly in Saha equilibrium.

## II. DIELECTRONIC RECOMBINATION RATES

Since DR is a resonant process, its rates and cross sections factorize, in the isolated resonance approximation, and can be given in terms of two building blocks, the autoionization and radiative decay probabilities, defined as  $A_a(a, b \rightarrow c, g) = 2\pi \langle a, b | V_{12} | c, g \rangle^2$  and  $A_r(a \rightarrow f) = 2\pi \langle f | \mathbf{e} \cdot \mathbf{r} | a \rangle^2$ , respectively. The doubly excited states will be denoted by  $R = (a, b)$ , and the initial state of the ion is taken to be its ground state  $g$ . For radiative decay, the  $a \rightarrow g$  transition is often the rapid mode. By exchange symmetry,  $b \rightarrow g$  and  $b \rightarrow f$  for singly excited final states  $f$ , etc., are also possible. In the isolated resonance approximation, where overlapping resonance terms are neglected, DR rates are given by

$$\begin{aligned} \alpha^{\text{DR}}(i \rightarrow R \rightarrow f) &= (4\pi R y / kT)^{3/2} (g_R / 2g_i) \\ &\quad \times \exp(-e_c / kT) A_a(R \rightarrow c, i) \\ &\quad \times A_r(R \rightarrow f) / (\Gamma_a + \Gamma_r). \end{aligned} \quad (2)$$

$\Gamma_a$  and  $\Gamma_r$  are the total Auger and radiative transition probabilities, respectively, for the resonance states ( $R$ ), and are given in terms of the  $A$ 's as  $\Gamma_r(R) = \sum_f A_r(R \rightarrow f)$  and  $\Gamma_a(R) = \sum_j A_a(R \rightarrow j)$ . Accurate  $\alpha$  can be evaluated once re-

liable  $A_a$  and  $A_r$  are available. They in turn depend critically on the various electronic wave functions involved in the matrix elements of the  $A$ 's.

It has been found convenient to categorize the DR process into three groups based on the different modes of excitation,  $g = (n_g, l_g) \rightarrow a = (n_a, l_a)$ , although this separation becomes less distinct as the number of open-shell electrons increases. This excitation is accompanied simultaneously by the capture of a continuum electron,  $c = (e_c, l_c) \rightarrow b = (n_b, l_b)$ , with the energy exchange between them. (Other permutations are also possible.) Then we have, with  $\Delta n \equiv n_a - n_g$  and  $\Delta l \equiv l_a - l_g$ , (i)  $\Delta n \neq 0$  involving intershell transitions, with large  $\Delta_{ag}$  and small  $n_b$  for orbital  $b$ ; (ii)  $\Delta n = 0, \Delta l \neq 0$  involving intrashell transitions, with moderate size  $\Delta_{ag}$  and  $n_b$ ; (iii)  $\Delta n = 0, \Delta l = 0$  involving intermultiplet transitions, with small  $\Delta_{ag}$  and large  $n_b$ .

The doubly excited resonance states formed by the initial step of excitation/capture in the DR process are affected by the plasma, due to the plasma microfield of the plasma ions, as well as any externally imposed electric and magnetic fields, and also by the collisional effects of plasma electrons. We denote these as plasma field distortions (PFD's) and plasma collisional transitions (PCT's), respectively. These two effects are not additive, however, and must be included in modeling of the plasma in a consistent way, without double counting. The outer-shell electrons in state ( $R$ ) with the principal quantum number  $n_b$  are in high Rydberg states for the excitation modes (ii) and (iii), and thus are most affected by the plasma effects.

Most of the data on DR rates available so far have been generated by a variety of theoretical methods and approximations, with varying degrees of accuracy. Since the work involved in the calculation of the rates is often complex and time consuming, much effort has been expended to developing procedures that are suited for each specific purpose, and several extensive computer codes are available. The theoretical method employed in the present study (Sec. IV) is dictated by the complexity of cascade contributions. We adopt the nonrelativistic distorted wave method for the continuum orbitals and model potential (or Hartree-Fock) treatment of the bound state orbitals in the evaluation of  $A_r$  and  $A_a$ . The simplest of the coupling schemes, the angular-momentum-averaged (AMA) scheme [5], is eminently suited for treating the complicated cascade effect. Generally, the final total rates tend to be overestimated by 20–30%.

For the discussion below, we define

$$\alpha_f^{\text{DR}}(i, f) = \sum_R \alpha^{\text{DR}}(g \rightarrow R \rightarrow f), \quad (3)$$

$$\alpha_R^{\text{DR}}(i, R) = \sum_f \alpha^{\text{DR}}(g \rightarrow R \rightarrow f), \quad (4)$$

and the total DR rate

$$\alpha_{\text{tot}}^{\text{DR}} = \sum_f \alpha^{\text{DR}}(i, f) = \sum_f \sum_R \alpha^{\text{DR}}(g \rightarrow R \rightarrow f). \quad (5)$$

As noted earlier, the last quantity defined by Eq. (5),  $\alpha_{\text{tot}}^{\text{DR}}$ , is routinely (and often inconsistently) used in almost all the past work in generating the empirical rate formulas. By con-

trast, DR experiments demonstrate the  $R$ -dependent cross sections  $\sigma_R^{\text{DR}}(i,R)$  and the rates  $\alpha_R^{\text{DR}}(i,R)$ . Sharp DR resonance peaks are observed as functions of the incident electron energy. Therefore, only the sum over  $f$  is required. For plasma modeling with the conventional form of the rate equations for the final excited state populations  $N(n)$ , the appropriate rates are  $\alpha_f^{\text{DR}}(i,f)$  defined by Eq. (3), and not  $\alpha_{\text{tot}}^{\text{DR}}$  of Eq. (5), where only the sum over  $R$  is performed. Evaluation of these new rates is rather more complicated, because several resonance states  $R$  can simultaneously contribute to the rates for the single final states  $f$ , via multiple cascades that require several generations of fluorescence yields. Calculation of  $\alpha_f^{\text{DR}}$  of Eq. (3) is slightly more involved than that performed previously for  $\alpha_{\text{tot}}^{\text{DR}}$ , but the final data are generated differently, by grouping the contributions to the individual final states, rather than by summing them all for the total rates.

The above discussion indicates that almost all the available DR rates are not useful for modeling purposes and a different set must be generated. However, some existing data can still be modified. In order to avoid unnecessary duplication of effort in generating the rates with specified final states, we briefly discuss the possibility of extracting the  $n$  dependence from the existing total rates. Here, the  $n$  ( $n = n_b$ ) dependence comes from the high Rydberg states  $b$  in  $R=(a,b)$ ; the orbital  $a$  is by our definition associated with low-lying states, and in the second step in Eq. (1) it is assumed that  $a \rightarrow g+x$ , while  $b$  are left in excited states; thus  $b \approx f$ . For the mode (i) process, the dominant contribution comes from states  $R$  in which both the orbitals  $a$  and  $b$  are low-lying excited states. Therefore, it is not likely that meaningful extraction of the  $n$  dependence from the existing total rates can be carried out, and different calculations will be necessary to estimate  $\alpha_{f=n}^{\text{DR}}(i,f=b=n)$  for the mode (i) case, as discussed in Sec. IV. On the other hand, for modes (ii) and (iii), high Rydberg state capture to orbital  $b$  is usually involved. The total rates are then obtained by summing the individual rates over  $n$ , assuming, e.g., the  $n^{-3}$  dependence for  $n \geq n_c$ , where  $n_c$  is the lowest  $n$  value allowed by energy conservation. [Here, as seen from Eq. (2),  $A_a < A_r$  for large  $n$  is assumed, where  $A_a \propto n^{-3}$  and  $A_r \propto \text{const}$ , independent of  $n$ . For  $A_a > A_r$ , we have  $\alpha \propto \text{const}$ , independent of  $n$ .] Therefore, for given total rates defined by  $\alpha_{\text{tot}}^{\text{DR}} = \sum_{n_c}^{\infty} \bar{\alpha}/n^3 \approx \bar{\alpha}/(2n_c^2)$ , we have  $\bar{\alpha} = 2n_c^2 \alpha_{\text{tot}}^{\text{DR}}$  and thus

$$\alpha_f^{\text{DR}}(i,n) \approx 2n_c^2 \alpha_{\text{tot}}^{\text{DR}}/n^3. \quad (6)$$

Of course, information on  $\alpha_{\text{tot}}^{\text{DR}}$  and  $n_c$  is assumed available. Equation (6) may eliminate the necessity of recalculation for modes (ii) and (iii) in some cases. Since the above suggested procedure depends on the explicit  $n$  dependence of the rates, the recent work of Ref. [6] may be of relevance.

### III. PLASMA EFFECTS: RATE EQUATIONS AND RATES

Modeling of plasmas requires setting up a realistic set of rate equations for the excited state population  $N(n,t)$  that include all the important atomic processes. The final state distribution is affected by the plasma collisional effect, which is treated by the rate equations. A complete set of DR

rates is needed, therefore, in addition to various other rates for the processes that are taking place inside the plasma. But, in spite of much effort over the past 30 years, the available data are far from complete. Empirical rate formulas are generated not only to summarize the vast amount of data in a compact and ready-to-use form, but also to interpolate for cases where the rates have not been explicitly calculated. As stressed above, they are exclusively for initial ground states of ions (i.e.,  $i=g$ ), and the contributions from  $f$  and  $R$  are summed, as indicated in Eq. (5). Furthermore, the plasma field effects are often important, especially for modes (ii) and (iii), but only a handful of cases have been analyzed, and no systematic compilation of data is currently possible.

Thus, the time evolution of a plasma toward quasiequilibrium is described by the rate equations for  $N(n,t)$ , where  $n$  denotes the quantum number of the singly excited final states ( $f$ ) of the recombined ions. Usually only the principal quantum number  $n$  is included, while the angular momenta associated with each  $n$  are averaged over, under the assumption that the collisional redistribution in the manifold is much faster than the other processes that are included explicitly in the rate equations. Thus, we have typically

$$\begin{aligned} dN(n)/dt = & - \left( N_e C_n^I + N_e \sum_{n' \neq n} C_{nn'} + \sum_{n' < n} A_{nn'} \right) N(n) \\ & + \left( N_e \sum_{n' \neq n} C_{n'n} + \sum_{n' > n} A_{n'n} \right) N(n') \\ & + N_e N_+ \alpha_n, \end{aligned} \quad (7)$$

where the upper limit of the sums is  $u > n, n' > g$ . The cutoff  $u$  represents the lowest Rydberg states that are in Saha equilibrium, while  $g$  denotes the ground state of the recombined ion. In Eq. (7),  $N_e$  and  $N_+$  are the free electron and ion densities, respectively.  $C^I$  denotes the collisional ionization rate for the ( $n \rightarrow c$ ) transition,  $C_{nm}$  are the collisional excitation/deexcitation rates for  $n \rightarrow m$ , and the  $A$ 's are the radiative decay rates ( $n \rightarrow n'$ ). The last term in the rate equations represents recombination processes, and is independent of  $N(n)$ , but instead depends on the ion density  $N_+$ , which is assumed to be that of the ground state; i.e., the recombination rates  $\alpha$  in Eq. (7) are given for ground state target ions. We have

$$\alpha_n = \alpha_n^{\text{RR}} + \alpha_n^{\text{TBR}} + \alpha_n^{\text{DR}}. \quad (8)$$

In view of the lack of data on the specific  $n$ -dependent rates  $\alpha_n^{\text{DR}}$ , the simple approximation is routinely made to replace the DR term, as follows:

$$N_e N_+ \alpha_n \rightarrow N_e N_+ \alpha_{\text{tot}} \delta_{n,g}. \quad (9)$$

Evidently, Eq. (9) is expected to become unreliable for plasmas with large  $N_+$  and at high temperature  $T$ . It is the purpose of this report to discuss the resolution of this problem, in terms of the  $n$  dependence of the final states. The  $g$  dependence of the initial ion will be the subject of a follow-up report.

Furthermore, previous work on modeling carbon impurities in a hydrogen plasma [7,8] has shown that at quasiequilibrium there is a substantial population of excited states of

the target ion, at the level of 5–10% of the ground state population. In determining the ionization balance that describes the degree of ionization as a function of temperature  $T$ , a pair of charge states  $Z^+$  and  $ZM^+$  are treated at a time, starting from  $Z=Z_c$  and proceeding to  $Z=0$ , where  $Z_c$  is the nuclear core charge. Thus, the solution of the rate equations for the pair  $Z^+$  and  $ZM^+$  should be the starting point of the next pair,  $ZM^+$  and  $(ZM-1)^+$ , etc. Obviously, the final state distribution at equilibrium for the recombined ion with  $ZM^+$  becomes the initial state of the “target ions” in the following step, with proper population distribution. Generally, the population of the excited ions  $N_+^{\text{equil}}(n)$  at equilibrium decreases rapidly with increasing  $n$ , up to a bottleneck around  $n=n_B \approx 4$ , and then gradually levels off to the Saha value. Therefore, when excited states of the target ion, before capture, are present in the plasma, the rate equations (7) must be modified by adding a term of the form

$$d(\Delta N)/dt = +N_e N_+^{(m)} \alpha_{nm}^e, \quad (10)$$

where the superscript  $m$  denotes the excited states of the target ion before capture. This extension of the model will be elaborated on elsewhere as a second part of this study. It turns out that the DR rates from the initial excited states of the target ions are quite large, larger by a factor of 3 to 10 as compared with DR from the ground state. In the present report, we limit our attempts to improving the approximation (9) by generating the  $n$ -dependent  $\alpha_n^{\text{DR}}$ . In connection with the PCT's, it is possible to approximately include a correction to the rates by using a specially tailored Fokker-Planck operator; the PCT modified rates  $\tilde{\alpha}$  may be obtained from  $\tilde{\alpha}^{\text{DR}(m)} \equiv (1 + \Omega) \alpha^{\text{DR}(m)}$ , where  $\Omega$  depends on the structure of the rate equations and rates. Some systematic studies of the plasma collisional and field effects have been made recently for a simplified hydrogen plasma with carbon impurities [2,8].

Discussion of DR in plasmas is not complete without touching on the other plasma effects, the PFD's, although the present study does not include this aspect. The presence of a field in the plasma affects the electron orbitals that are involved in the DR process, thus affecting the rates. The static ion microfield for the PFD is represented, for example, by the Holtzmark field, or time-dependent refinements can be made [2,9]. In addition to the electric field effect, a combination of an electric and magnetic field may further modify the above result [10]. This may be viewed as producing an extra electric field in the Lorentz transformed drift frame with velocity  $\vec{u} = c\mathbf{E} \times \mathbf{B}/E^2$ ; the change in the electric field may be approximately  $\Delta\mathbf{E} = B^2\mathbf{E}/2E^2$ .

The PCT and PFD effects are in general not additive. A previous study [8] takes this problem into account by first modifying the rates under the PFD, and then inserting them into the rate equations for the PCT's. The result seems to indicate that possible interference between the two effects is small. However, much more work is needed to clarify the situation.

#### IV. DR RATES AND FINAL STATE DISTRIBUTION

In this section, we illustrate the importance of the dependence of the DR rates on the final excited states of the re-

combined ions, by explicit calculation of the rates for the ground state of Ne-like  $\text{Al}^{3+}$  target ions. All the dominant intermediate resonance states are considered, and the results compared with the conventional total DR rates. As pointed out earlier, the total rates are often summarized by various forms of empirical formula. Thus, for example, in one recent report [14], a set of empirical formulas was obtained by fitting separately for each excitation mode (i) and (ii). The rates for mode (iii) have not been tabulated; they are important only at low temperature, but the problem of PFD can be serious, and getting an empirical formula for them may be difficult. As discussed in Sec. III, the task of extracting the  $n$  dependence associated with the final recombined states ( $f$ ) from the available total rates for mode (ii) may be possible without direct recalculation of the rates. Therefore, we concentrate below on the rates that involve the excitation mode (i). A simple distorted wave method is adopted here, with single-configuration Hartree-Fock wave functions for the bound state orbitals, and in the angular-momentum-averaged coupling scheme, mainly because of complicated cascade effects that need to be taken into account. As will become obvious, any other refined procedures make the calculation nearly intractable.

The DR rates for  $\text{Al}^{3+}$  calculated here explicitly depend on the final states ( $f$ ), and the contributions from different resonance states ( $R$ ) to the same individual final states are summed in the isolated resonance approximation. Even with these simplifications, the calculation is very complicated, due to the presence of multiple cascade transitions. (To simplify notation, explicit reference to the core  $1s^2 2s^2$  is omitted for all the configurations.) The initial state of the target ion is  $i = 2p^6$ . All  $R$  states of the general form  $2p^5 3snl$ ,  $2p^5 3pnl$ , and  $2p^5 3dnl$  are investigated in detail, up to  $n=6$ . The calculated  $\alpha_n^{\text{DR}}$  are presented in three groups,  $A$ ,  $B$ , and  $C$ , depending on the number of maximum allowed Auger channels (1, 2, and 3, respectively). Group  $A$  includes all the  $R = 2p^5 3snl$  states, which are allowed to autoionize by Auger-electron emission to the ground state  $2p^6$  only. Group  $B$  contains  $R$  states of the form  $2p^5 3pnl$ , which may Auger decay to both  $2p^6$  and  $2p^5 3s$   $n \geq 5$ . The group  $B$  states have small  $\alpha^{\text{DR}}$  values because the Auger rates to  $2p^5 3s$  are at least 10 times larger than that to  $2p^6$ . In addition,  $3p$  states are not dipole allowed to decay radiatively to the  $2p^5$  orbital. Group  $C$  deals with  $2p^5 3dnl$  states; the  $d$  state  $2p^5 3d^2$  can autoionize only to the  $2p^6$  final state. However, a subgroup of  $R$  states  $2p^5 3d4l$  may Auger decay to both  $2p^6$  and  $2p^5 3s$  final states. Moreover, starting from  $n=5$ ,  $2p^5 3dnl$  can Auger decay also to  $2p^5 3p$ , where the  $2p^5 3p$  Auger rate is much larger than the other rates, including the small radiative channel with width  $\Gamma_r$ . Thus, the contribution of group  $C$  to the total  $\alpha^{\text{DR}}$  is small at  $n=4$  and decreases rapidly for  $n \geq 5$ . In the following, we denote the singly excited, Auger-stable final states by  $f_m$ ; all other states reached in the intermediate steps of cascades are denoted by  $k_m$ .

Since the calculation of the rates that involve multiple cascades is complicated, we illustrate the problem by presenting a simple typical example of the distribution of  $\alpha^{\text{DR}}$  over final singly excited states. Consider the decay scheme of the  $R \equiv 2p^5 3s5f$  state created by the first step of DR, as

TABLE I. DR rates in units of  $10^{-14}$  cm<sup>3</sup>/sec for group A intermediate states  $2p^53snl$  of Al<sup>3+</sup>.  $kT=3.7$  Ry. The numbers in brackets are additive powers of ten to  $10^{-14}$ , e.g.,  $0.55[-2]$  means  $0.55 \times 10^{-2}$  in the above units, i.e.,  $0.55 \times 10^{-16}$  cm<sup>3</sup>/sec.

<i>R</i>	<i>f</i>																
	<i>n</i> =3			<i>n</i> =4				<i>n</i> =5			<i>n</i> =6						
	3 <i>s</i>	3 <i>p</i>	3 <i>d</i>	4 <i>s</i>	4 <i>p</i>	4 <i>d</i>	4 <i>f</i>	5 <i>s</i>	5 <i>p</i>	5 <i>d</i>	5 <i>f</i>	5 <i>g</i>	6 <i>s</i>	6 <i>p</i>	6 <i>d</i>	6 <i>f</i>	6 <i>g</i>
3 <i>s</i> <sup>2</sup>	0.75																
3 <i>s</i> 3 <i>p</i>	5.5[-3]	4.15															
3 <i>s</i> 3 <i>d</i>	6.33	0.2[-2]	5.39														
3 <i>s</i> 4 <i>s</i>	0.16	2.6[-4]		0.73													
3 <i>s</i> 4 <i>p</i>	1.9[-3]		2.9[-4]		3.41												
3 <i>s</i> 4 <i>d</i>	2.51	1.5[-5]				5.66											
3 <i>s</i> 4 <i>f</i>	5.1[-3]		4.4[-3]				6.76										
3 <i>s</i> 5 <i>s</i>	5.6[-2]	7.9[-5]			1.3[-4]			0.65									
3 <i>s</i> 5 <i>p</i>	1.2[-3]		8.4[-5]			3.3[-4]			3.39								
3 <i>s</i> 5 <i>d</i>	1.23		1.0[-6]		4.5[-5]		1.5[-3]			5.55							
3 <i>s</i> 5 <i>f</i>	2.8[-3]		1.7[-3]			1.7[-3]					6.71						
3 <i>s</i> 5 <i>g</i>	9.8[-6]		8.3[-6]				1.3[-2]					1.95					
3 <i>s</i> 6 <i>s</i>	2.2[-2]	3.1[-5]		4.1[-5]					8.7[-5]				0.52				
3 <i>s</i> 6 <i>p</i>	7.3[-4]		3.9[-5]			9.8[-5]				2.8[-4]				3.36			
3 <i>s</i> 6 <i>d</i>	0.69				0.5[-5]		6.2[-4]								5.53		
3 <i>s</i> 6 <i>f</i>	1.6[-3]		8.3[-4]			9.8[-4]				0.8[-3]						6.38	
3 <i>s</i> 6 <i>g</i>	4.1[-6]		3.3[-6]				5.5[-3]				4.5[-3]						1.87
Subtotal		21.3				16.6				18.3					17.7		

TABLE II. Same as Table I, but for group *B* states  $2p^5pnl$  of  $\text{Al}^{3+}$ . All the rates that are less than  $10^{-19}$   $\text{cm}^3/\text{sec}$  are omitted from the table for simplicity.

<i>R</i>	<i>n</i> =3			<i>f</i>		<i>n</i> =5	
	3 <i>s</i>	3 <i>p</i>	3 <i>d</i>	4 <i>s</i>	4 <i>d</i>	5 <i>s</i>	5 <i>d</i>
3 <i>p</i> <sup>2</sup>	0.14[−4]	0.11[−1]					
3 <i>p</i> 3 <i>d</i>	0.68[−2]	17.97	0.59[−2]				
3 <i>p</i> 4 <i>s</i>	0.24[−1]	0.91		0.112			
3 <i>p</i> 4 <i>d</i>	0.62[−2]	6.73			0.15[−1]		
3 <i>p</i> 5 <i>s</i>	0.81[−4]	0.21[−2]				0.95[−3]	
3 <i>p</i> 5 <i>d</i>	0.61[−4]	0.38[−1]					0.34[−3]
Subtotal		25.7			0.127		0.13[−2]

$$\begin{aligned}
 2p^6+k_c l_c \rightarrow 2p^5 3s 5f &\rightarrow 2p^6 5f \quad (k_1) \\
 (i) \quad (d) &\rightarrow 2p^5 3s 3d \quad (k_2) \\
 &\rightarrow 2p^5 3s 4d \quad (k_3). \quad (11)
 \end{aligned}$$

The values of Auger rates  $A_a$  at the allowed  $l_c$  values are  $A_a(l_c=2)=0.2137[10] \text{ sec}^{-1}$  and  $A_a(l_c=4)=0.2816[11] \text{ sec}^{-1}$ . (The number in brackets denotes the power of 10.) The radiative rates to dominant final states  $k_1$ ,  $k_2$ , and  $k_3$  are found to be  $A_{r1}=0.4341[10]$ ,  $A_{r2}=0.584[9]$ , and  $A_{r3}=0.188[9] \text{ sec}^{-1}$ . Thus, the Auger, radiative, and resonance widths are  $\Gamma_a(d)=0.3029[11]$ ,  $\Gamma_r(d)=0.5113[10]$ , and  $\Gamma(d)=0.354[11]$ , all in  $\text{sec}^{-1}$ . The radiationless capture probability is  $V_a=0.2545[13] \text{ sec}^{-1}$ . The fluorescence yield for the first final singly excited state  $k_1=f_1=(2p^6 5f)$  is  $\omega(2p^6 5f)=A_{r1}/\Gamma(d)=0.1226$ . Using Eq. (2), the DR rate for this  $k_1$  is then

$$\alpha^{\text{DR}}(2p^6 5f)=6.71[-14] \text{ cm}^3/\text{sec}. \quad (12)$$

In the second step, state  $k_2$  is still Auger unstable and will decay again by either Auger or radiative transition as

$$2p^5 3s 5f \rightarrow 2p^5 3s 3d \rightarrow 2p^6 3d \rightarrow 2p^6 3s, \quad (13)$$

where  $\omega_1=0.165[-1]$ ,  $\omega_2=0.188[-2]$ , and  $\omega_3=0.221[-2]$ . Therefore  $\omega(2p^6 3d)=\omega_1 \times \omega_2=0.31[-4]$  and thus

$$\alpha^{\text{DR}}(2p^6 3d)=0.169[-16] \text{ cm}^3/\text{sec}. \quad (14)$$

On the other hand, with  $\omega(2p^6 3s)=\omega_1 \times \omega_3=0.364[-4]$ , we obtain

$$\alpha^{\text{DR}}(2p^6 3s)=0.199[-16] \text{ cm}^3/\text{sec}. \quad (15)$$

In addition,  $k_3$  decays also by  $A_a$  or by  $A_r$  as

$$2p^5 3s 5f \rightarrow 2p^5 3s 4d \rightarrow 2p^6 4d \rightarrow 2p^6 3s, \quad (16)$$

where  $\omega_4=0.53[-2]$ ,  $\omega_5=0.59[-2]$ , and  $\omega_6=0.26[-2]$ . Thus,  $\omega(2p^6 4d)=\omega_4 \times \omega_5=0.313[-4]$ , and this gives

$$\alpha^{\text{DR}}(2p^6 4d)=0.76[-17] \text{ cm}^3/\text{sec}. \quad (17)$$

We also have  $\omega(2p^6 3s)=\omega_4 \times \omega_6=0.139[-4]$ , and hence

$$\alpha^{\text{DR}}(2p^6 3s)=0.76[-17] \text{ cm}^3/\text{sec}. \quad (18)$$

The DR rate for the state  $(2p^6 3s)$  can be obtained by adding the values of  $\alpha^{\text{DR}}$  in Eqs. (15) and (18):

$$\alpha^{\text{DR}}(2p^6 3s)=0.275[-16] \text{ cm}^3/\text{sec}. \quad (19)$$

Hence, the final state distribution of the DR rate for  $R=2p^5 3s 5f$  is given by Eqs. (12), (14), (17), and (19).

Table I summarizes all the important distributions from group *A* ( $2p^5 3snl$ ). Here, two points must be stressed: (i) The final states with very small values of  $\omega$ , which may be reached as a third step of cascade decays, are neglected to simplify the example. (ii) For some *R* states, final excited states are reached by at least four routes of decay. Thus, the distribution of DR rates over the final excited states must be calculated carefully through all available routes. It is obvious from the table that the main contribution to  $\alpha^{\text{DR}}$  of  $f=2p^6 3l$  comes from  $R=2p^5 3s 3l$  states. Similarly, the main contribution to  $\alpha^{\text{DR}}$  of  $f=2p^6 4l$  is from  $2p^5 3s 4l$  states, and so on. The DR rate at  $n=5$  is slightly greater than that at  $n=4$ , an unexpected result. This may be attributed to the presence of resonance states *R* with 5*g*, since no such *g* orbital is allowed at  $n=4$ . In addition, in the  $\text{Al}^{3+}$  case the  $3s \rightarrow 2p^5$  radiative transition dominates at all  $n$  in the decay of  $2p^5 3snl$ . However, at  $n=6$  the DR rate starts to decrease slowly and is predicted to scale as  $1/n^3$  from  $n=7$ , because it will behave mainly as the Auger rate to the ground state. Hence, the high Rydberg states (HRS) contributions are estimated using an empirical formula of the type of Eq. (6).

In Table II, we present the calculated DR rates associated with group *B* ( $2p^5 3pnl$ ) intermediate states. The *R* states  $2p^5 3p 3d$  and  $2p^5 3p 4d$  have large DR rates, where they are allowed energetically to autoionize to the  $2p^6$  ground state only. However, all  $2p^5 nl$  with  $n \geq 5$  are allowed to autoionize to both  $2p^6$  and  $2p^5 3s$  states. Therefore, DR rates are suddenly decreased as we go from  $n=4$  to  $n \geq 5$ . In addition, both 3*d* or 4*d* orbitals in the states  $2p^5 3p 3d$  or  $3p 4d$  strongly decay radiatively to  $2p^6$  state. Thus, DR rates to  $2p^6 3p$  dominate the contribution from group *B* states, especially  $3p 3d$  and  $3p 4d$ . On the other hand, all states of the form  $2p^5 3p np$  have very small DR rates because either 3*p*

TABLE III. Same as in Table II, but for group  $C$   $2p^5 3dnl$  states. The DR rates for  $n=6$  are very small due to the  $2p^5 3p$  Auger decay channel, which opens up at  $n=5$ .

$R$	$f$											
	$n=3$			$n=4$				$n=5$				
	$3s$	$3p$	$3d$	$4s$	$4p$	$4d$	$4f$	$5s$	$5p$	$5d$	$5f$	$5g$
$3d^2$	4.2[-5]	1.2[-1]	19.95									
$3d4s$		6.0[-5]	5.2[-3]	2.6[-2]								
$3d4p$	7.4[-6]		7.2[-4]	4.4[-6]	2.8[-1]							
$3d4d$	0.5[-5]	2.8[-3]	6.6[-1]			3.52						
$3d4f$			1.2[-4]				7.8[-2]					
$3d5s$		5.9[-6]	4.7[-4]		3.4[-6]			7.7[-3]				
$3d5p$			2.9[-6]			3.7[-6]			2.8[-2]			
$3d5d$		1.6[-3]	2.7[-2]				7.3[-4]			2.5[-1]		
$3d5f$			4.4[-6]			2.5[-6]					6.9[-3]	
$3d5g$							6.4[-6]					8.6[-4]
Subtotal		20.8			3.9					0.3		

or  $np$  orbitals are not allowed to stabilize radiatively, in the dipole approximation, to the  $2p^5$  orbital.

The values of  $\alpha^{\text{DR}}$  in units of  $10^{-14}$  cm<sup>3</sup>/sec for group  $C$  ( $2p^5 3dnl$ ) states are presented in Table III. In this group, the  $R$  states with  $n=3$ , i.e.,  $3d^2$ , radiatively decay only to  $2p^6$ , while  $3d4l$  may autoionize to  $2p^5 3s$  as well. Therefore, the DR rate for  $3d4d$  decreases by as much as a factor of 6 from that for  $2p^5 3d^2$ . The  $R$  states  $2p^5 3d5l$  are allowed also to autoionize to  $2p^6 3p$  with large  $A_a$  values and thus the DR rates for group  $C$  states are very small at  $n \geq 5$ , as seen in Table III.

In summary, from Tables I–III, we note that the main contributions to  $2p^6 3l$  are from  $2p^5 3s3l$ ,  $3p3d$ , and  $3p4d$  as well as  $3d^2$  and  $3d4d$ , and all other  $R$  states in groups  $B$  and  $C$  have very small DR rates for  $n \geq 5$ . The final state distribution with relatively large DR rates is from  $2p^5 3snl$ ,  $n \geq 4$ . This situation is expected to be completely different for ions with a higher degree of ionization in the Ne isoelec-

tronic sequence, e.g., Fe<sup>16+</sup>, where the values of  $n$  in  $R$  states at which the Auger channels  $2p^5 3s$  and  $2p^5 3p$  open up become larger. Typically, for the Fe<sup>16+</sup> case with group  $B$  and  $C$  states, the transitions to  $2p^5 3s$  take place at  $n=10$  and  $7$ , respectively. This leads to the formation of the final state  $f=2p^6 nl$  with  $3 \leq n \leq 9$  and large DR rates; more specifically, the  $R$  states  $2p^5 3pnl$  ( $n=3-9$ ) and  $2p^5 3dnl$  ( $n=3-6$ ) are involved.

We summarize the result of Tables I–III in Table IV for ready comparison. The three rows for each entry of  $R$  give the DR rates at temperatures of 1.85, 3.7, and 7.4 Ry. The group of resonance states  $2p^5 3snl$  formed from the initial target in its ground state is dominant for all values of  $n$  of the final excited states  $2p^6 nl$ . (However, these  $3snl$  states are not allowed to be formed if the initial states are not the ground state.) The HRS contribution is large and comes mostly from  $3snl$ ,  $n > 5$ . On the other hand, the HRS contributions from  $R=3pnl$  and  $3dnl$  groups are negligible.

TABLE IV. DR rates in units of  $10^{-14}$  cm<sup>3</sup>/sec summarized for the three groups of resonance states  $R = 2p^5 3snl$ ,  $2p^5 3pnl$ , and  $2p^5 3dnl$ . The electron temperature  $T$  is chosen around the maximum at  $kT \approx (2/3)e_c$ ; the continuum electron energy is close to 5 Ry for the present system of Al<sup>3+</sup>; we also treat the cases with  $kT=1.85, 3.7, \text{ and } 7.4$  Ry. The final states  $f=2p^6 nl$ .

$R$	$kT$ (Ry)	$f$					Total
		$n=3$	$n=4$	$n=5$	$n=6$	$n>6$	
$3snl$	1.85	16.4	11.5	12.0	11.2	24.6	75.7
	3.7	21.3	16.6	18.3	17.7	38.9	112.8
	7.4	14.5	11.8	13.4	13.2	29.0	81.9
$3pnl$	1.85	16.0	8.1[-2]	8.2[-4]		1.8[-3]	16.1
	3.7	25.7	1.3[-1]	1.3[-3]		2.9[-3]	25.8
	7.4	19.4	9.5[-2]	9.7[-4]		2.1[-3]	19.5
$3dnl$	1.85	10.0	1.9	1.4[-1]		3.1[-1]	12.4
	3.7	20.8	4.1	2.9[-1]		6.4[-1]	25.8
	7.4	17.8	3.3	2.6[-1]		5.7[-1]	21.9
Total	1.85	42.4	13.5	12.1	11.2	24.9	104.2
	3.7	67.8	20.8	18.6	17.7	39.5	164.4
	7.4	51.7	15.2	13.7	13.2	29.6	123.3

Finally, we note that the contributions from all the  $R = 4lnl'$  states with  $n > 3$  are negligible when the initial state is the ground state  $i = 2p^6 = g$ , because there are strong Auger channels that result in  $2p^5 3s$ ,  $2p^5 3p$ , and  $2p^5 3d$  as well as the Auger decay to  $g$ .

## V. SUMMARY

We have pointed out the need to extend the existing empirical formulas for the DR rates to be explicitly dependent on the final recombined states. This modification is consistent with the rate equations to which DR and many other rates are to be introduced. The existing empirical formulas for the total DR rates are not applicable to the rate equations that determine the excited state population  $N(n)$  of the recombined ions. We emphasize several points of some importance in generating the DR rates for modeling plasmas.

(1) The DR rate formulas must be generated in such a way that the final singly excited states are explicitly specified. This requires a slight adjustment of the conventional procedure adopted in detailed benchmark calculations. The total rates summed over all the singly excited final states must be used only in the limit of very low plasma densities.

(2) The DR rates for the initial excited states are also

desirable, but have rarely been considered. This requires a serious extension of the conventional rate equations, and will be the subject of discussion in a future publication [11]. Overall consistency requires such an extension.

(3) From the several existing benchmark calculations [12–14] and their adjusted results, a different set of rate formulas may be generated. In some cases, the existing total rates [15] for the excitation mode (ii), and perhaps also for mode (iii), may be used to approximately extract the  $n$  dependence, as the high- $n$  contributions may often be known to be either constant independent of  $n$  or of the  $n^{-3}$  type.

(4) The DR rates associated with the excitation modes (ii) and (iii) are especially sensitive to external field perturbations. Systematic compilation of data that include the PFD effect is yet to be carried out.

## ACKNOWLEDGMENTS

This work was supported in part by the Egyptian Cultural Bureau in the U.S.A. and by the University of Connecticut. G.O. would like to thank the Physics Department of the University of Connecticut for hospitality and use of the computer facility.

- 
- [1] *Recombination of Atomic Ions*, Vol. 296 of *NATO Advanced Study Institute, Series B: Physics*, edited by W. Graham *et al.* (Plenum Press, New York, 1992).
- [2] Y. Hahn, *Rep. Prog. Phys.* **60**, 691 (1997).
- [3] G. H. Dunn, in *Recombination of Atomic Ions* (Ref. [1]) gives an up-to-date review.
- [4] Y. Hahn (unpublished).
- [5] Y. Hahn, *Adv. At. Mol. Phys.* **21**, 123 (1985).
- [6] J. Wang, T. Kato, and I. Murakami, *Phys. Rev. A* **60**, 2104 (1999).
- [7] D. B. Riesenfeld, *Astrophys. J.* **398**, 386 (1992).
- [8] J. Li and Y. Hahn, *Z. Phys. D: At., Mol. Clusters* **41**, 19 (1997).
- [9] Y. Hahn and K. LaGattuta, *Phys. Rep.* **166**, 195 (1988).
- [10] F. Robicheaux and M. S. Pindzola, *Phys. Rev. Lett.* **79**, 2237 (1997); T. Bartsch *et al.*, *ibid.* **82**, 3779 (1999).
- [11] G. Omar and Y. Hahn (unpublished).
- [12] H. L. Zhang, S. N. Nahar, and A. K. Pradhan, *J. Phys. B* **32**, 1459 (1999).
- [13] D. W. Savin *et al.*, *Astrophys. J.* **523**, 855 (1999).
- [14] S. N. Nahar, M. A. Bautista, and A. K. Pradhan, *Phys. Rev. A* **58**, 4593 (1998); S. N. Nahar and M. A. Bautista, *Astrophys. J., Suppl. Ser.* **120**, 327 (1999); E. Behar *et al.*, *Phys. Rev. A* **54**, 3070 (1996).
- [15] Y. Hahn, *J. Quant. Spectrosc. Radiat. Transf.* **49**, 81 (1993); **51**, 663(E) (1994); **41**, 315 (1989); *Numerical Data and Functional Relationships in Science and Technology*, edited by Y. Itikawa, Landolt-Börnstein, New Series, Group I, Vol. 17 (Springer-Verlag, Berlin, 1999).